Journal of Mechanical Science and Technology 25 (1) (2011) 61~68
www.springerlink.com/content/1738-494x
DOI 10.1007/s12206-010-1102-0

Comparison of collocation strategies of sensor and actuator for vibration control †

Young-Sup Lee*
Department of Embedded Systems Engineering, University of Incheon, Incheon, 406-772, Korea

(Manuscript Received October 1, 2009; Revised June 28, 2010; Accepted October 8, 2010)

Abstract

Some possible collocation strategies of sensor and actuator pairs for the application to active vibration control systems are analyzed, compared and discussed in this paper. This is becausea well-designed sensor - actuator collocation configuration can provide a simpler control algorithm with excellent performance and stability, especially when velocity feedback is adopted. As an ideal point collocation pair of a sensor and actuator shows high possibility in actual vibration control problems, the advantage of a collocated accelerometer - shaker pair is proven experimentally and discussed first. Then as a similar approach, a collocated piezosensor - piezoactuator pair is analyzed in depth with the in-plane motion coupling. Finally, two configurations of a practically collocated configuration with an accelerometer - piezoactuator pair and a non-overlapped collocated pair of a bimorph piezosensor - two bimorph piezoactuators are described in detail in terms of performance and stability with experimental results. Those two configurations are expected for the applications to more practical active control of vibration systems with the velocity feedback control scheme.

Keywords: Collocation of sensor and actuator; Control stability; Velocity feedback; Vibration control; Piezoelectric actuator

1. Introduction

Collocation configuration of sensor and actuator pairs has been one of important factors in active control of vibration in various structures. This is because control algorithm, performance and stability can be varied by the collocation configuration [1-4].

It is well-known that an ideally collocated pair of a point sensor and actuator with velocity feedback strategy offers an extremely robust active feedback control system [2]. This strategy is unconditionally stable for any type of primary disturbance acting on a structure, in spite of having a very simple controller. In the case of non-collocated systems, the trade-off between stability and performance is critically important because better stability usually causes the degradation of performance [5, 6].

Since the development of the active vibration control system, for example, a restricted number of outputs are available commercially even though there have been many promising results in laboratories [4, 7, 8]. The following are some of the main reasons for that: the requirement for a large number of sensors and actuators, complicated centralized multichannel input and output controllers, and increased weights and costs [6-8]. It is noted, by the way, that the demand for "realistic active control systems" has been still high from industry customers.

Smart materials such as piezoelectric transducers have been widely used as actuators, sensors, or self-sensing actuators especially in active vibration control and active structural acoustical control [7-10].

In this study, dynamic responses and properties of some practically implementable collocated sensor - actuator pair configurations including conventional shakers, accelerometers and piezoelectric transducers will be analyzed and discussed in detail. Hence, this paper targets ultimately to implement a simpler, smaller and more realistic analog active control system, which consists of sensors, actuators and power amplifiers without digital signal processors and low pass filters.

Section 2 of this paper describes the theoretical background of the configuration of a collocated sensor and actuator pair and velocity feedback control strategy for active control of vibration. Section 3 discusses sensor - actuator response results with a collocated pair of accelerometer - shaker attached on a beam. Section 4 shows the theoretical analysis and experimental results of a collocated in a wide area or *matched* pair of a piezosensor and piezoactuator configuration. Another practically collocated pair configuration with an accelerometer and piezoactuator is mentioned in detail at section 5. In section

† This paper was recommended for publication in revised form by Associate Editor Dong Hwan Kim
*Corresponding author. Tel.: +82 32 835 8656, Fax.: +82 32 835 8760
E-mail address: ysl@incheon.ac.kr

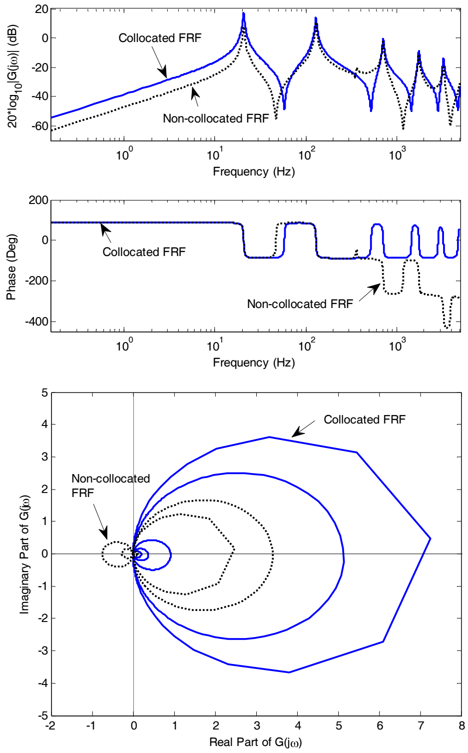

Fig. 1. Responses of a collocated pair and a non-collocated pair of ideal point velocity sensor and actuator system. *Top*: Sensor - actuator frequency responses. *Bottom*: Nyquist plots.

6, a new configuration with a non-overlapped collocated pair of a bimorph piezosensor and two bimorph piezoactuators is discussed with computer simulation for the application to active vibration control in terms of performance and stability.

2. Theoretical background for collocation

Consider two identical cantilever beams with a pair of *ideal* point collocated sensor - actuators on a beam and a pair of non-collocated point sensor - actuators on the other. If an ideal point actuator excites the beam at x_a and an ideal velocity sensor detects out-of-plane motion at x_s, the out-of-plane velocity field $\dot{w}(x_s,t)$ of the beam is expressed as [11]

$$\dot{w}(x_s,t) = \sum_{n=1}^{\infty} \phi_n(x_s) \frac{\partial}{\partial t} q_n(x,t) , \tag{1}$$

where $\phi_n(x_s)$ is the nth out-of-plane mode shape and $q_n(x,t)$ is the corresponding modal coordinate. The frequency response of the beam with the collocated pair can be expressed, $\omega \in (-\infty, +\infty)$, as

$$G_c(j\omega) = \frac{\dot{w}(x_s,\omega)}{f(x_a,\omega)} = \sum_{n=1}^{\infty} \frac{j\omega\phi_n^2(x_s)}{M_n[(\omega_n^2 - \omega^2) + j2\zeta_n\omega_n\omega]} , \tag{2}$$

where $x_a = x_s$, ω_n is the nth natural frequency, ς is the viscous damping ratio, M_n is the nth modal mass and $f(x,\omega)$ is the forcing function. On the contrary, the frequency response of the beam with the non-collocated pair when $x_a \neq x_s$ is expressed with

$$G_{nc}(j\omega) = \frac{\dot{w}(x_s,\omega)}{f(x_a,\omega)} = \sum_{n=1}^{\infty} \frac{j\omega\phi_n(x_a)\phi_n^T(x_s)}{M_n[(\omega_n^2 - \omega^2) + j2\zeta_n\omega_n\omega]} . \tag{3}$$

Computer simulation results of two identical cantilever beams (aluminum, $L \times B \times T$ = 200 × 30 × 1 mm) are plotted for the collocated pair (solid lines) and the non-collocated pair (dotted lines) in Fig. 1. As it can be seen from top of Fig. 1, the sensor - actuator response of the collocated pair shows that the magnitude of each resonance is decreasing with the increase of frequency and the resonances and anti-resonances are alternating, and the phase response stays between $\pm 90^\circ$. However, the response of the non-collocated pair shows that some anti-resonances have disappeared and the phase response doesn't stay between $\pm 90^\circ$.

From the bottom of Fig. 1, the Nyquist plot for the collocated pair is displayed only on the positive real part region, but that of the non-collocated part is plotted both on the positive and negative real parts regions.

As shown in Eqs. (2) and (3), the denominator part of the transfer function consists of the infinite number of complex conjugate pairs of *system poles*, indicating the resonances due to the vibration modes, which are determined by boundary conditions and material properties of the beam. However, the numerator part of the function is determined by the locations of the actuator and sensor, and this represents that the numerator determines the *system zeros* and influences the phase relation between the system input (actuator) and output (sensor) [5]. Thus, the phase response is decided by the location of sensor and actuator.

The non-collocation of a sensor and actuator introduces the *unstable zeros* and it makes the system *non-minimum phase*, which can be defined as "a system for which some, but not all, of the complex conjugate pairs of zeros are located in the right hand side on the *s*-plane" [12]. The stability of the closed-loop velocity feedback system of a non-collocated pair with a feedback gain of $H(j\omega) = h$ can be determined. The closed-loop system must be unstable if the feedback gain h is greater than a critical value.

On the contrary, the collocation of sensor and actuator makes the system *minimum phase*, which can be defined as "a system for which all the complex conjugate pairs of poles and zeros are located in the left hand side on the *s*-plane" [12].

As a special case of a minimum phase system, *strictly positive real* (SPR), which can be defined as "a system for which all the complex conjugate pairs of poles and zeros are alternating each other as well as located in the left hand side on the *s*-plane" [6,12]. This indicates alternating resonances and anti-resonances are displayed in the collocated sensor - actuator frequency response as can be seen from Fig. 1 (solid lines at the top). Also, the real part of the frequency response of such a system of $G(j\omega)$ is always greater than zero for all frequen-

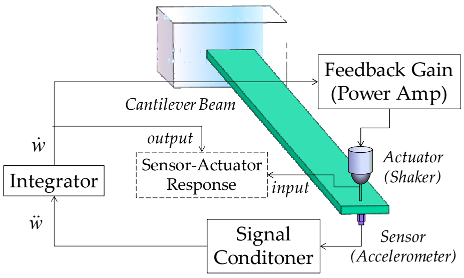

Fig. 2. Velocity feedback control with a collocated pair of sensor (accelerometer)-actuator (shaker) on a cantilever beam.

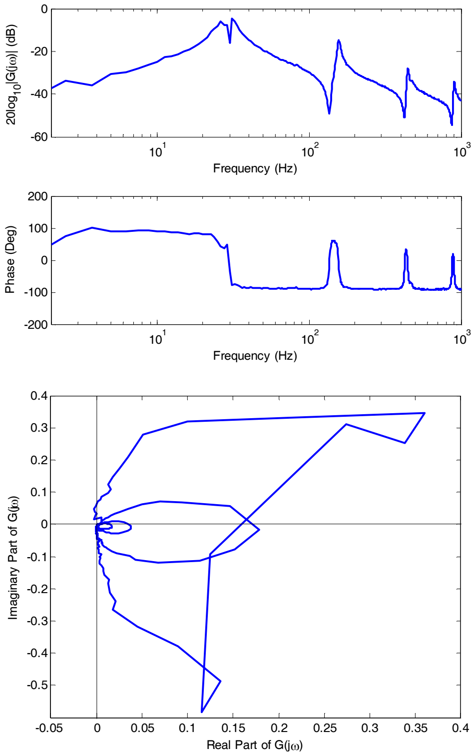

Fig. 3. Measured response of a practically collocated system with a shaker and accelerometer. *Top*: Sensor - actuator frequency response. *Bottom*: Nyquist plot.

cies, and can be written as $\mathrm{Re}[G(j\omega)] > 0$ [6]. Thus, the SPR condition provides a very important requirement in the design of unconditionally stable control system based on velocity feedback scheme with a constant gain.

3. Practical collocation

3.1 Accelerometer and shaker

As shown in Fig. 2, a pair of sensor (accelerometer, B&K 4375) and actuator (shaker, B&K 4810) is installed to be collocated ($x_a = x_s$) on the tip of an experimental cantilever beam (aluminum, $L \times B \times T$ = 200 × 30 × 1 mm). The signal from the accelerometer is integrated by a signal conditioner to give velocity information $\dot{w}(x_s, \omega)$ at the beam tip. The accelerometer - shaker response was measured and analyzed with a frequency analyzer.

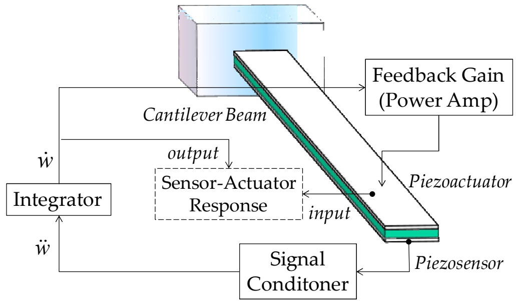

Fig. 4. A matched pair of distributed sensor - actuator system on a cantilever beam.

The measured sensor - actuator frequency response function (FRF) of the beam is plotted in Fig. 3 (top). Since the sensor and actuator are collocated, the response shows a typical SPR response property with the decreasing trend of resonance magnitudes, alternating resonances and anti-resonances, and phase response staying between $\pm 90^\circ$. Also the Nyquist plot of the response is presented in Fig. 3 (bottom) and it indicates that the real parts of the response are positive.

From this response, if velocity feedback control scheme is applied as shown in Fig. 2, a powerful active vibration control can be implemented as long as a pair of an accelerometer and shaker is collocated. The sensor - actuator pair generates a proper control force with a feedback gain h which is proportional to the velocity of the beam at the sensor location [1]. Thus, this arrangement can give the effect as if a *skyhook damper* is installed at $x_a = x_s$ on the beam.

3.2 Piezosensor and piezoactuator

Although the configuration in section 3 provides nice properties for velocity feedback control, it requires a quite large space to install the shaker onto the structure. So a smart material such as piezoelectric PZT (piezoelectric zirconate titanate) or PVDF (piezoelectric vinylidene fluoride) is considered to minimize the space.

A *matched* (collocated on a wide area) pair of PVDF piezosensor and piezoactuator bonded on either side of a cantilever beam (aluminum, L × B × T = 200 × 30 × 1 mm) is implemented as shown in Fig. 4, which is inspired from the collocated pair of an accelerometer and shaker described in section 3 to utilize such an attractive SPR response property when it is implemented with the velocity feedback strategy [8, 13].

It is known that a piezoactuator bonded on a beam can excite the beam both to the in-plane (longitudinal) and the out-of-plane (flexural) directions. The strain of the piezosensor ε_x within linear elasticity due to the deformation can be expressed with [9, 10]

$$\varepsilon_x = \frac{\partial}{\partial x}\left(u - h_{sen}\frac{\partial w}{\partial x}\right) = \frac{\partial u}{\partial x} + \left(-h_{sen}\frac{\partial^2 w}{\partial x^2}\right), \tag{4}$$

where u , w and h_{sen} are the longitudinal displacement, flexural displacement, and the distance between the neutral

Table 1. Values of the coefficients and symbols for the aluminium beam.

Coefficients	Values	Remarks
Beam [mm]	200 × 30 × 1	Aluminium
Piezoactuator [mm]	200 × 30 × 0.5	PVDF
Piezosensor [mm]	200 × 30 × 0.5	PVDF
ζ_n	0.05	
h_{sen} [mm]	0.75	
C_{oop}	8.3929 * 10^{-8}	
C_{ip}	3.5826 * 10^{-5}	
M_n	0.0162	Modal mass

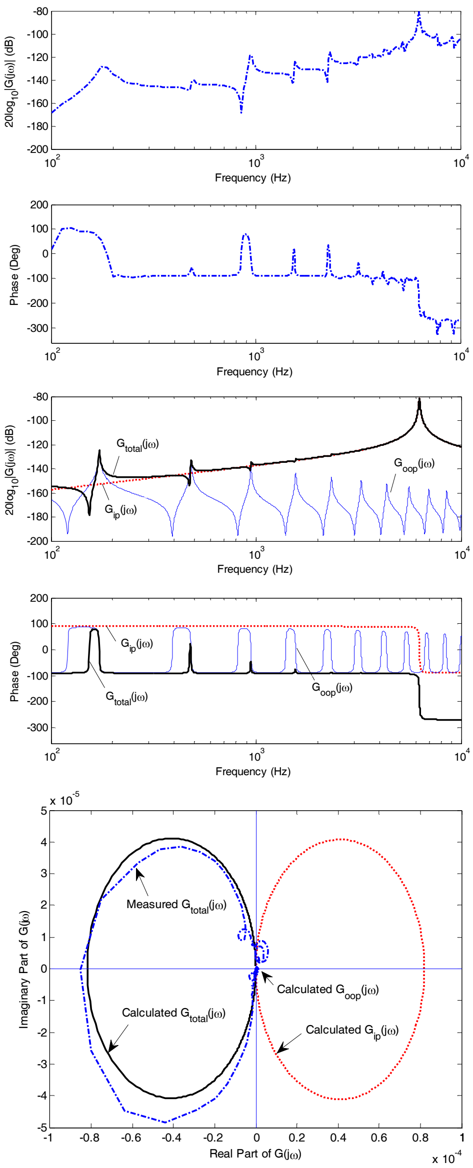

Fig. 5. Comparison of the measured and calculated FRFs between the matched sensor - actuator pair. *Top*: Measured total FRF $G_{total}(j\omega)$. *Middle*: Calculated total FRF $G_{total}(j\omega)$, out-of-plane FRF $G_{oop}(j\omega)$, and in-plane FRF $G_{ip}(j\omega)$. *Bottom*: Nyquist plots.

axis of the beam and the sensor respectively. Thus, the total electrical charge output $q_{total}(t)$ from the piezosensor is the *addition* of the out-of-plane portion $q_{oop}(t)$ and the in-plane one $q_{ip}(t)$, $q_{total}(t) = q_{oop}(t) + q_{ip}(t)$, and each of them can be written as [10]

$$q_{oop}(t) = -e_{31} h_{sen} B \int_0^L S(x,y) \frac{\partial^2 w}{\partial x^2} dx ,$$
$$q_{ip}(t) = e_{31} B \int_0^L S(x,y) \frac{\partial u(x,t)}{\partial x} dx , \tag{5}$$

where $e_{31} = 6.55$ [$\mathrm{NV^{-1}m^{-1}}$ or $\mathrm{CN^{-1}}$] is a piezoelectric constant, B is the width of the beam and $S(x,y)$ is the shape function of the piezosensor. The total transfer function between the input voltage $V_3(t)$ to the piezoactuator and the time-derivative of charge output $i = dq/dt$ of the piezosensor, which is equivalent to velocity signal $\dot{w}(x_s, \omega)$ of a collocated pair, can be written as

$$G_{total} = i_{oop} / V_3 + i_{ip} / V_3 = G_{oop} + G_{ip} , \tag{6}$$

where G_{oop} and G_{ip} are the transfer functions for the out-of-plane and in-plane motions, respectively, and they can be expressed in terms of FRF after some manipulation as

$$G_{oop}(j\omega) = j\omega \frac{C_{oop}(j\omega)}{V_3(j\omega)} \sum_{n=1}^{\infty} \frac{[\phi_n'(L) - \phi_n'(0)]^2}{M_n[(\omega_n^2 - \omega^2) + 2j\zeta\omega_n\omega]} ,$$
$$G_{ip}(j\omega) = -j\omega \frac{C_{ip}(j\omega)}{V_3(j\omega)} \sum_{m=1}^{\infty} \frac{[\int_0^L \psi_m(x) dx]^2}{[(\omega_m^2 - \omega^2) + 2j\zeta\omega_m\omega]} , \tag{7}$$

where C_{oop}, C_{ip} are coefficients related to the electromechanical coupling between piezoelectric transducers and the beam. The symbols' values are given in Table 1; $\phi'(x)$ is the derivative of $\phi(x)$ with respect to x, and $\phi(x)$ and $\psi(x)$ are the flexural and longitudinal mode shapes, respectively.

Fig. 5 (*top*) is the measured FRF of the matched sensor - actuator pair and shows a strange sensor - actuator response with increasing trend of the resonances, a huge resonance at around 6,000 Hz caused by the first in-plane mode, not alternating resonances and anti-resonances, and phase response not staying between $\pm 90^\circ$. It is clearly different from that of the accelerometer - shaker pair in Fig. 3. This can be explained because, according to Eq. (6), the matched pair of piezosensor - piezoactuator cannot avoid the coupled motion of both the out-of-plane and in-plane motions.

As plotted in Fig. 5 (*middle*), the calculated total response G_{total} (thick line) consists of not only the calculated out-of-plane response G_{oop} (thin line) but also the calculated in-plane response G_{ip} (dotted line), that is, $G_{total} = G_{oop} + G_{ip}$. It indicates that the coupled FRF G_{total} loses the SPR response property due to the first in-plane resonance where the phase undergoes a sudden 180° shift. The Nyquist plots in Fig. 5 (*Bottom*) also show the total response whether it is measured

Table 2. Values of the coefficients and symbols for the aluminium beam.

Coefficients	Values	Remarks
Beam [mm]	200 × 20 × 2	Aluminium
Piezoactuator [mm]	15 × 20 × 1	PZT5H
ζ_n	0.05	
C_M	9.2977 * 10^{-6}	
M_n	0.0216	Modal mass

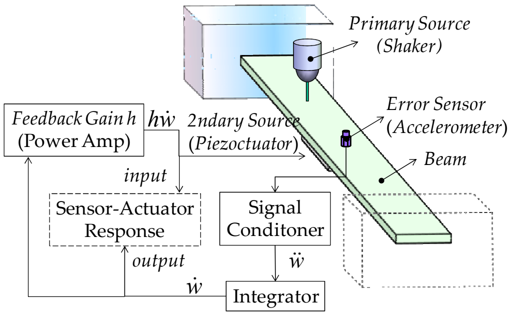

Fig. 6. An accelerometer and piezoactuator pair configuration on a beam for active vibration control with velocity feedback.

or calculated has negative real parts that can cause instability with a high feedback gain.

Hence, the configuration with a matched pair of piezosensor and piezoactuator is not feasible for velocity feedback control scheme.

3.3 Accelerometer and piezoactuator

As an alternative to the matched piezosensor - piezoactuator pair, a *practically collocated* pair of an accelerometer and piezoactuator installed on a clamped-clamped beam (aluminum, $L \times B \times T = 200 \times 20 \times 2$ mm) is implemented as shown in Fig. 6 in order to eliminate the in-plane motion only from the coupled motion so that purely out-of-plane motion can be obtained.

Since the accelerometer is assumed to be located at x_s which is the center of the opposite side of the piezoactuator, it detects the flexural velocity at x_s of the beam. The FRF of the sensor - actuator pair, when the output is the velocity signal and the input is the voltage applied to the piezoactuator, can be expressed as

$$G(j\omega) = \frac{\dot{w}(x_s,\omega)}{V_3(\omega)} = j\omega C_M \sum_{n=1}^{\infty} \frac{\phi_n(x_s)[\phi_n'(x_1) - \phi_n'(x_2)]}{M_n[(\omega_n^2 - \omega^2) + j2\zeta\omega_n\omega]} \quad , \quad (8)$$

where x_1 and x_2 are both ends of the piezoactuator patch and $x_s = (x_1 + x_2)/2$, and C_M is a coefficient related to electromechanical coupling and its and other symbols' values are given in Table 2.

Actually, the accelerometer (PCB 352C66) and piezoactuator (PZT5H) pair are *practically* collocated with x_s = 100 mm, x_1 = 92.5 mm and x_2 = 107.5 mm for experiment.

The measured sensor - actuator FRF is plotted in Fig. 7

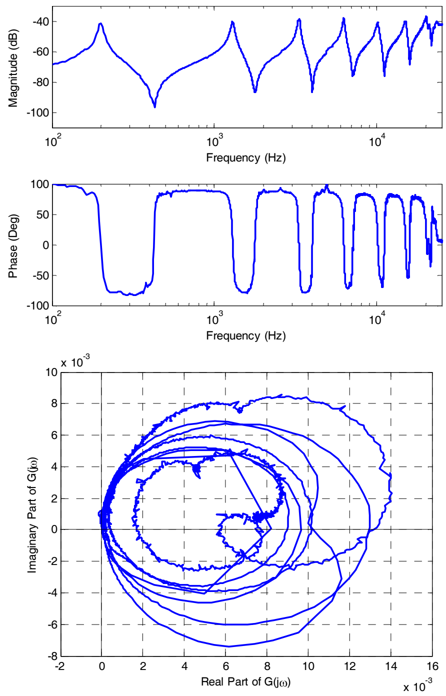

Fig. 7. *Top*: Measured sensor - actuator FRF of an accelerometer - piezoactuator pair. *Bottom*: Nyquist plot.

(top). It shows an SPR response with alternating resonances and anti-resonances up to 12,000 Hz while the phase response exists between ±90°. The Nyquist plot in Fig. 7 (bottom) shows the measured response is positive real below 12,000 Hz.

Thus as long as the accelerometer is attached on the opposite *center* of the piezoactuator, that is, $x_s = (x_1 + x_2)/2$, no matter where x_1 and x_2 are, and the piezoactuator length is shorter than the 1/2 wavelength of the highest vibration mode to be controlled, the real part of the sensor - actuator FRF is always positive *below a certain frequency*, for example 12,000 Hz in this case. It means that some negative real parts can be observed if the frequency is higher than 12,000 Hz in which the sensor and the actuator are *not in-phase*. So this configuration is a practical approach to remove the in-plane coupling problem below a reasonably high frequency.

Also, since the magnitudes of the resonances are getting smaller in higher frequencies generally, even if the negative real parts in a high frequency range exist they usually cannot threaten control stability. By the way, in this case, it has not been observed clearly the decreasing trend of the resonance magnitudes like that of the collocated accelerometer - shaker pair as shown in Fig. 3 (*Top*). This is because the PZT piezoactuator generates not out-of-plane force but bending moments at both ends of itself [7, 8, 10]. So the maximum allowable feedback gain would be limited with this configuration than the accelerometer - shaker configuration.

It is also noted that the velocity feedback control with this pair of sensor and actuator is a kind of all mode control not a specific mode control. Thu,s it controls not only odd modes but also the even modes.

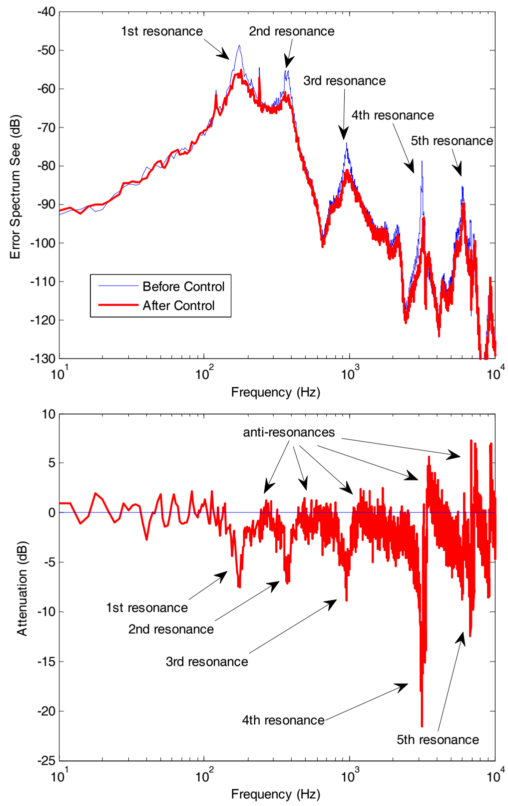

Fig. 8. Results of accelerometer - shaker configuration before and after control with velocity feedback (gain margin = 6 dB). *Top*: Comparison of measured error spectra. *Bottom*: Attenuation.

For the active vibration control experiment using velocity feedback scheme, the feedback gain $H(j\omega)=h$ was adjusted to make the open-loop response stable with 6 dB gain margin, and the error signal from the accelerometer is integrated by a signal conditioner PCB 441A101 to give the velocity output. Then the velocity signal is transferred via a PCB Power Amplifier 790 for the feedback gain h to generate voltage which is proportional to velocity for driving the piezoactuator as a secondary source. A primary source (shaker, B&K 4810) was installed at 50 mm away from one of the clamped ends to generate disturbance to the beam as shown in Fig. 6.

The error power spectra $S_{ee}(f)$ before and after control are plotted in Fig. 8 (*Top*), where the reduction of about 8, 7 and 9 dB at 1st, 2nd and 3rd resonance, respectively, especially 22 dB at the 4th resonance near 3000 Hz.

In velocity feedback, since the control force by the piezoactuator is proportional to the velocity measured by the accelerometer, the piezoactuator produces a pair of bending moments $m_s(x_1)=-m_s(x_2)\ =-C_M h\dot{w}(x_s)$, where C_M is defined in Eq. (8). This is derived from the fact that the bending moment due to the electric voltage V_3 (t) applied to the piezoactuator, can be defined as "moment = constant * voltage". In velocity feedback control, the sensor signal $\dot{w}(x_s)$ is fed back and multiplied by the negative feedback gain $-h$, then the amplified signal $-h\dot{w}(x_s)$ is transferred to the piezoactuator to make the bending moments. It is noted that the force generated by this *accelerometer - piezoactuator* pair is an anti-phased bending moments pair; however, the collocated *accelerometer - shaker* pair is an anti-phased linear force to suppress vibration of a structure.

As shown in Fig. 8 (bottom), the magnitude attenuation of error spectrum after control is illustrated and it indicates velocity feedback control with the practically collocated accelerometer - piezoactuator configuration worked very well to suppress the beam vibration.

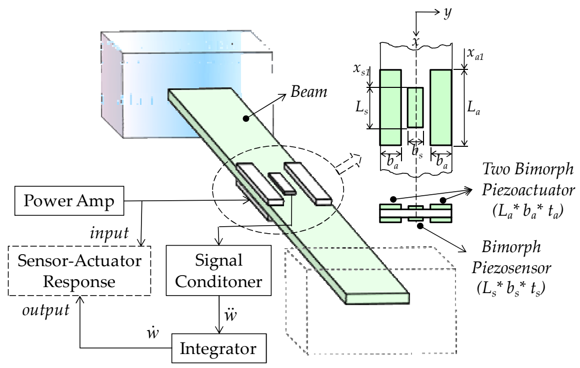

Fig. 9. A non-overlapped collocated pair of a bimorph piezosensor and two bimorph piezoactuators to remove the in-plane coupling of a beam.

3.4 Non-overlapped bimorph piezosensor and p iezoactuator

Another alternative to the matched piezosensor - piezoactuator pair, a *non-overlapped collocated* pair of a *bimorph* piezosensor and two *bimorph* piezoactuators is considered as shown in Fig. 9 in order to utilize the merits of piezoelectric transducers.

A set of bimorph piezoactuator ($L_a \times b_a \times t_a$), which extends from x_{a1} to x_{a2} from one end of the beam, can generate pure out-of-plane motion of the beam if the actuator set is bonded and operated *out-of-phase*. The out-of-phase bimorph piezoactuator set can cancel the in-plane motion of the beam. Two sets are applied to the beam in order to generate more actuation force. The out-of-phase bimorph piezosensor ($L_s \times b_s \times t_s$), which is bonded from x_{s1} to x_{s2} from one end of the beam, consists of two piezosensor patches as shown in Fig. 9.

The longitudinal middle point of the piezosensor and piezoactuator must be the same, as $x_m=(x_{s1}+x_{s2})/2=(x_{a1}+x_{a2})/2$ for this configuration. Thus, for this piezosensor and piezoactuator configuration it is expected that the in-plane coupling would be removed from total response.

The charge output from this piezosensor can be defined as

$$q(t)=2e_{31}h_{sen}\int_{-b_s/2}^{b_s/2}\int_{x_{s1}}^{x_{s2}} S(x)\frac{\partial^2 w}{\partial x^2}dxdy\,. \tag{9}$$

Thus, after some manipulation, the sensor - actuator FRF of this configuration can be obtained as

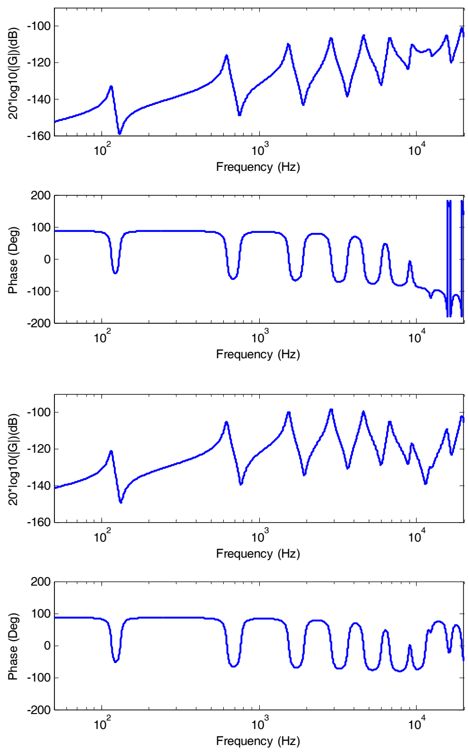

Fig. 10. Calculated sensor - actuator responses of a non-overlapped collocated system with a bimorph piezosensor and two bimorph piezoactuators. *Top*: Response when the collocated length is a quarter of the piezoactuator length. *Bottom*: Response when the collocated length is identical to the piezoactuator length.

$$G(j\omega) = j\omega \frac{C(j\omega)}{V_3(j\omega)} \cdot \sum_{n=1}^{\infty} \frac{[\phi_n'(x_{s2}) - \phi_n'(x_{s1})][\phi_n'(x_{a2}) - \phi_n'(x_{a1})]}{M_n[(\omega_n^2 - \omega^2) + 2j\zeta\omega_n\omega]}, \tag{10}$$

where C is a coefficient related to the electromechanical coupling between the piezosensor - piezoactuator pair and the beam.

In computer simulation results of this configuration with a clamped-clamped beam (steel, $L \times B \times T$ = 300 × 30 × 2 mm) are displayed in Fig. 10. In this simulation, the critically important SPR response for velocity feedback scheme is investigated. Also, the effect of the sensor length variation is considered for better control performance and stability.

As can be seen from Fig. 10 (top), when the length of the piezosensor is L_s = 10 mm (a quarter of the piezoactuator length L_a) the SPR response property collapses at about 10,000 Hz because of collocated length of the sensor and actuator is less small. However, when the collocated length is increased to make $L_s = L_a$, the SPR response property continues at least up to 20,000 Hz as plotted in Fig. 10 (bottom). The simulation results show that this configuration using only piezoelectric transducers could provide a powerful SPR property in a wider frequency range and allows an increased feedback gain with velocity feedback scheme compared to the accelerometer - piezoactuator pair configuration.

Even though a more precise manufacturing process is necessary to implement this sensor - actuator configuration, it could become one of nice choices to suppress unwanted vibration.

4. Conclusions

This paper describes a comparison of practically possible three different configurations of sensor and actuator pairs in terms of performance and stability to implement realistic active control systems for vibration suppression with velocity feedback scheme. Theoretical and experimental results discussed in this paper can be summarized as the following:

First, a collocated pair of an accelerometer and shaker is very nice in terms of performance and stability with SPR response, but the volume and mass of the shaker restricts its applications to vibration control of smart structures. This pair can give a skyhook damper effect when it is operated with velocity feedback control scheme.

Second, a matched pair of a piezosensor and piezoactuator is not relevant to an active vibration control system especially when velocity feedback scheme is applied because of the in-plane coupling problem which can cause instability. This configuration cannot offer an SPR response.

Third, a practically collocated pair of an accelerometer and piezoactuator allows implementing a vibration control system that can maintain SPR response within a reasonable frequency range. This configuration provides good performance and reasonably high stability for the implementation of an active vibration control system with velocity feedback scheme.

Fourth, a non-overlapped collocated pair of a bimorph piezosensor and two bimorph piezoactuators could provide a response free from in-plane coupling and is expected to offer another good choice for better control performance and stability with the same scheme.

Acknowledgment

This work was supported by the University of Incheon Research Grant in 2008.

References

[1] M. J. Balas, Direct Velocity Feedback Control of Large Space Structures, *Journal of Guidance and Control*, 2 (3) (1979) 252-253.

[2] J. Q. Sun, Some observations on physical duality and collocation of structural control sensors and actuators, *Journal of Sound and Vibration*, 194 (5) (1996) 765-770.

[3] Y.-S. Lee, P. Gardonio and S. J. Elliott, Coupling analysis of a matched piezoelectric sensor and actuator pair for vibration control of a smart beam, *Journal of Acoustical Society of America*, 111 (6) (2002) 2715-2726.

[4] A. Preumont, *Vibration Control of Active Structures: An Introduction* (2nd Ed.), Kluwer Academic Publishers (2002).

[5] G. F. Franklin, J. D. Powell and A. Emami-Naeini, *Feedback Control of Dynamic Systems* (3rd ed.), Addison-Wesley (1994).
[6] S. J. Elliott, *Signal Processing for Active Control*, Academic Press (2001).
[7] C. R. Fuller, S. J. Elliott and P. A. Nelson, *Active Control of Vibration*, Academic Press (1996).
[8] R. L. Clark, W. R. Saunders and G. P. Gibbs, *Adaptive Structures Dynamics and Control*, John Wiley & Sons (1998).
[9] Y.-S. Lee, S. J. Elliott and P. Gardonio, Matched piezoelectric double sensor/actuator pairs for beam motion control, *Smart Materials and Structures*, 12 (4) (2003) 541-548.
[10] Y.- S. Lee, *Active Control of Smart Structures using Distributed Piezoelectric Transducers*, PhD Thesis, University of Southampton (2000).
[11] D. J. Mead, *Passive Vibration Control*, John Wiley & Sons (1999).
[12] A. V. Oppenheim and R. W. Schafer, *Discrete-Time Signal Processing*, Prentice Hall (1989).
[13] M. E. Johnson and S. J. Elliott, Active control of sound radiation using volume velocity cancellation, *Journal of Acoustical Society of America*, 98 (4) (1995) 2174-2186.

Young-Sup Lee received his BS degree in Naval Architecture from Pusan National University, Korea, in 1987. He then received his MSc and PhD degrees from University of Southampton, United Kingdom, in 1997 and 2000, respectively. Dr. Lee is currently an associate professor at Department of Embedded Systems Engineering in University of Incheon, Korea. Dr. Lee's research interests include active control of sound and vibration, signal processing, and smart sensors and actuators.